Eur. Phys. J. B **13**, 297–303 (2000)

THE EUROPEAN PHYSICAL JOURNAL B

EDP Sciences
© Società Italiana di Fisica
Springer-Verlag 2000

Experimental evidence and consequences of rare events in quantum tunneling

V. Da Costa[a], Y. Henry, F. Bardou, M. Romeo, and K. Ounadjela

Institut de Physique et Chimie des Matériaux de Strasbourg[b], 23 rue du Loess, 67037 Strasbourg Cedex, France

Received 1 April 1999

Abstract. Tiny spatial fluctuations of tunnel barrier parameters are shown to have dramatic consequences on the statistical properties of quantum tunneling. A direct experimental evidence is provided that the tunnel current through metal-oxide junctions, imaged at a nanometric scale, exhibits broad statistical distributions extending over more than 4 orders of magnitude. Striking effects of broad current distributions are shown: the total tunnel transmission is dominated by few highly transmitting sites and the typical current density varies strongly with the size of the junction. Moreover, self-averaging of the tunnel current fluctuations occurs only for unexpectedly large junction areas.

PACS. 05.40.-a Fluctuation phenomena, random processes, noise, and Brownian motion – 73.40.Gk Tunneling – 73.40.Rw Metal-insulator-metal structures

A profound theory of broad statistical distributions was developed by the statistician Paul Lévy in the 30's [1]. However, it is only recently that broad distributions have attracted for themselves much interest in physics [2]. Although this is often ignored, such distributions are expected to be a ubiquitous feature. They are indeed identified in more and more processes from turbulent flows and dynamical chaos to laser cooling of atomic gases. Their striking features among which the statistical domination by rare events and specific scaling behaviors are becoming key ideas of modern statistical physics. While the basic properties of quantum tunneling are known since the early days of quantum mechanics, important and non-trivial features arise when introducing ingredients such as dissipation [3], Coulomb blockade [4] or disorder. The effects of disorder on quantum tunneling were first considered when inspiring theoretical studies [5] predicted that some low temperature properties of glasses were to be attributed to hypothetical broad distributions of the tunneling probability of atoms resulting from the topological disorder. Relaxation measurements subsequently provided ample support to these predictions [6]. More recently, broad distributions of tunneling rates showed up in amorphous polymers [7,8] and in the transport properties of 1D disordered semiconductors [9].

While these studies were confined to low temperatures, broad distributions are likely to show up more generally in any process combining tunneling and disorder, such as electron transfer in proteins [10], nuclear fusion in inhomogeneous plasmas and electron transport through thin oxide films. Thin oxide films are relatively simple 2D systems, of practical importance as they are frequently used to make tunnel junctions. They are becoming a key technological issue as the sizes of the CMOS transistors shrink. Moreover, the field of tunnel junctions has recently been enriched by the discovery that devices consisting of two ferromagnetic metal films separated by an oxide insulating layer exhibit giant magnetoresistance effects at room temperature [11].

In this paper, we show that thin metal-oxide films offer a unique opportunity to measure directly and at room temperature the spatial fluctuations of the tunnel current at a nanometric scale. The current distributions, attributed to rather small spatial fluctuations of tunnel barrier parameters (such as thickness or barrier height), are shown to be extremely broad, as predicted in reference [12]. This is in marked contrast with the narrow distributions of ohmic currents collected from oxide free metal films. We point out some striking consequences of the occurrence of broad current distributions. The total conductance is dominated by tunneling through very few localized sites, rare events which are reminiscent of Lévy flights, and the typical current density varies dramatically with the size of the junction.

The tunnel currents through metal-oxide junctions were successfully imaged with a nanometric resolution by combining Atomic Force Microscopy (AFM) with *simultaneous* local current measurements [13]. By scanning a conducting tip placed in *contact* with the sample, we simultaneously recorded a topographical image and a current image. The topography was obtained by standard AFM carried out in contact and constant force (a few nN) mode. Concurrently, a bias voltage of typically 1 V was applied

[a] e-mail: `victor@michelangelo.u-strasbg.fr`
[b] UMR 7504 CNRS - Université Louis Pasteur.

between the bottom metal layer and the conducting tip to generate a current flow from the sample to the probe. This produced a cartography of the electrical features of the sample surface, which proved to be highly reproducible. The probes used in this study are common Si_3N_4 insulating cantilevers with integrated pyramidal tips, which were coated with 30 nm thick ultrahard TiN_x conducting films.

Three kinds of samples were studied, all of them having been prepared in conditions which allowed to obtain smooth top surfaces. The first type of samples consisted of 25 nm thick epitaxial hcp (0001) Ru films deposited on mica substrates by ultrahigh vacuum *e*-beam evaporation. When studied shortly after deposition, these films proved to have oxide free top surfaces. The second type of samples consisted of superficially oxidized, 10 nm thick hcp (0001) Co films grown on single crystal Ru buffer layers. The oxidation of the top Co surface was accomplished by leaving the films under atmospheric conditions. Finally, the third type of samples consisted of sputtered (2 nm)Co/AlO_x junctions. To minimise the roughness of the oxide films, these junctions were grown on (2 nm)Cr/(3 nm)Fe/(30 nm)Cu buffer layers previously deposited on (111) Si substrates. The top metallic Al layer, 1 nm in nominal thickness, was oxidized *in situ* in an oxygen glow discharge plasma for 60 s. The Al oxide layer, mainly made of Al_2O_3, was characterized using X-ray Photoemission Spectroscopy (XPS). This allowed to adjust the oxidation conditions so as to avoid the formation of Co oxide and/or the presence of residual metallic Al.

Figure 1 shows typical topographical and current images recorded simultaneously while scanning an oxide free Ru surface (Figs. 1a and 1b, 500×500 nm^2, 256×256 pixels, 1 V), a Co oxide surface (Figs. 1c and 1d, 150×150 nm^2, 512×512 pixels, 1 V) and an Al oxide surface (Figs. 1e and 1f, 150×150 nm^2, 512×512 pixels, 1.3 V). The topographical images of Figures 1c and 1e reveal that both plasma oxidation and natural oxidation lead to rather smooth top surfaces with height standard deviations of 0.1 nm for Al oxide and 0.5 nm for Co oxide. The red (respectively blue) zones in the current images of Figures 1d and 1f correspond to high (respectively low) tunneling currents and hence to sites where the thickness or the height of the tunnel barrier might be locally smaller (respectively larger) than the average value. Note that no obvious correlation exist between the topographical and electrical data, as can be clearly seen from a comparison of the height and current profiles of Figure 1.

To firmly establish the physical nature of the collected currents, local current-voltage measurements were performed using the same setup with the tip at rest. The fact that the current carriers were actually tunneling through continuous, *pinhole free*, Co and Al oxide overlayers was ascertained as we measured strongly non-linear i–V characteristics (Figs. 2c and 2e) at different sites of the samples surface including the sites with the highest currents where the tunnel transmission approaches 10^{-5} [14]. The same experiments carried out on oxide free Ru films revealed linear i–V curves (Fig. 2a) that, beyond the metallic character of the Ru films, clearly demonstrate the ohmic behavior of the probe conductivity and hence the absence of significant oxide contamination on the tip apex. Also, these linear i–V curves indicate that the water film that possibly covers the samples is locally removed in the probe/sample contact region due to the pressure exerted by the tip.

From the current images, we calculated the statistical distribution of local currents $P_i(i)$. As a general trend, current maps recorded on superficially oxidized metal films and oxide free metal films show drastic quantitative as well as qualitative differences. This is illustrated in Figures 2b, 2d and 2f showing the current distributions computed from the current images displayed in Figure 1. The current distribution associated with the metallic Ru surface (Fig. 2b) exhibits a *narrow Gaussian* shape with an average value of 11.4 μA and a small standard deviation of only 1.6 μA: the current thus flows in a rather homogeneous way through the Ru layer. In contrast, the distributions of tunnel current obtained for the Co and Al oxide surfaces (Figs. 2d and 2f) are extremely *broad*. They show strongly asymmetric shapes with pronounced maxima (at 12 pA and 270 pA respectively) and very slow decreases for large currents. From these distributions which extend from very small or undetectable values ($\lesssim 1$ pA) to about 100 nA, it appears that the tunnel current can vary from place to place by more than 4 orders of magnitude and that relatively high currents are only transmitted through very few sites. The spatial fluctuations of tunnel currents are also clearly evidenced in the current profiles of Figures 1d and 1f.

The occurrence of broad distributions for the current tunneling through *imperfect* potential barriers was anticipated by a recent statistical analysis [12] briefly recalled here. One considers the effect of the spatial fluctuations of barrier thickness that unavoidably exist in real junctions. The distribution of barrier thickness l is assumed to be Gaussian with an average value $\langle l \rangle$ and a small standard deviation $\sigma_l \ll \langle l \rangle$. The probability t for a particle of mass M and kinetic energy E to tunnel through a rectangular potential barrier of height V_0 and thickness $l \gg \lambda$ is given by $t = 4A\exp(-l/\lambda)$ where $\lambda = \hbar/(2\sqrt{2M(V_0 - E)})$ is the attenuation length in the barrier and $A = 4E(V_0 - E)/V_0^2$. This leads to a log-normal distribution $P_t(t)$ of the transmission t

$$P_t(t) = \frac{1}{\beta\sqrt{2\pi}}\frac{1}{t}\exp\left[-\frac{1}{2\beta^2}\left(\ln(t) - \alpha\right)^2\right] \qquad (1)$$

where $\alpha = \ln(4A) - \langle l \rangle/\lambda$ is a scale parameter and $\beta = \sigma_l/\lambda$ is a fluctuation parameter. Since we measured local currents i and not local transmissions t, we introduce a proportionality factor η such that $t = \eta i$. This linear transformation leads to a current distribution $P_i(i) = \eta P_t(\eta i)$ which writes as equation (1) with a new scale parameter $\alpha' = \alpha - \ln(\eta)$ but the same fluctuation parameter β.

Depending on β which is proportional to the barrier fluctuations, $P_i(i)$ presents qualitatively very different behaviors. For small β, $P_i(i)$ is close to a usual narrow (Gaussian) distribution, whereas for large β,

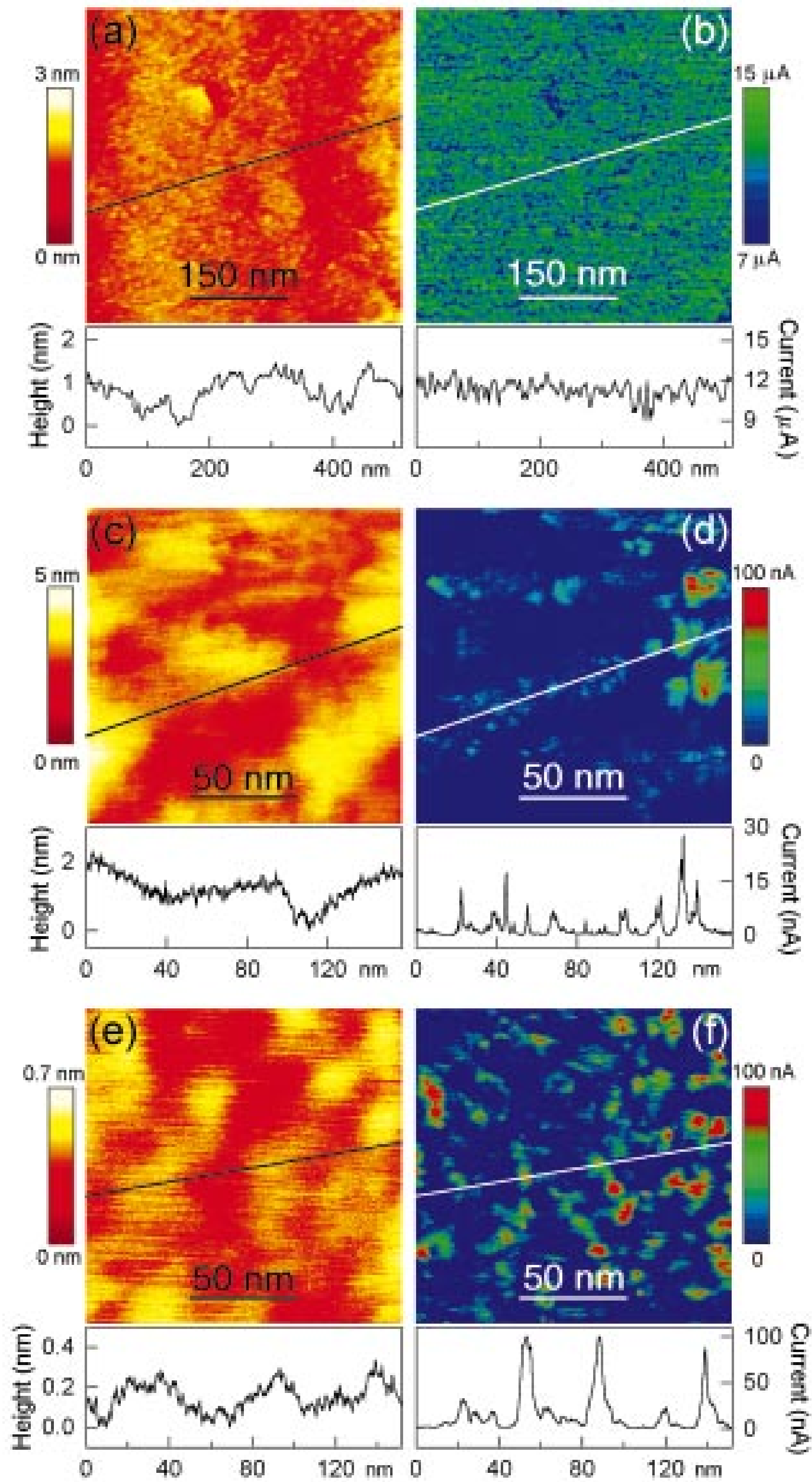

Fig. 1. (a, c, e) Topographical and (b, d, f) current images of the surface of an oxide free Ru film (a, b), a naturally oxidized Co film (c, d) and a plasma oxidized Al film (e, f). Also displayed are height and current profiles along lines shown in the images.

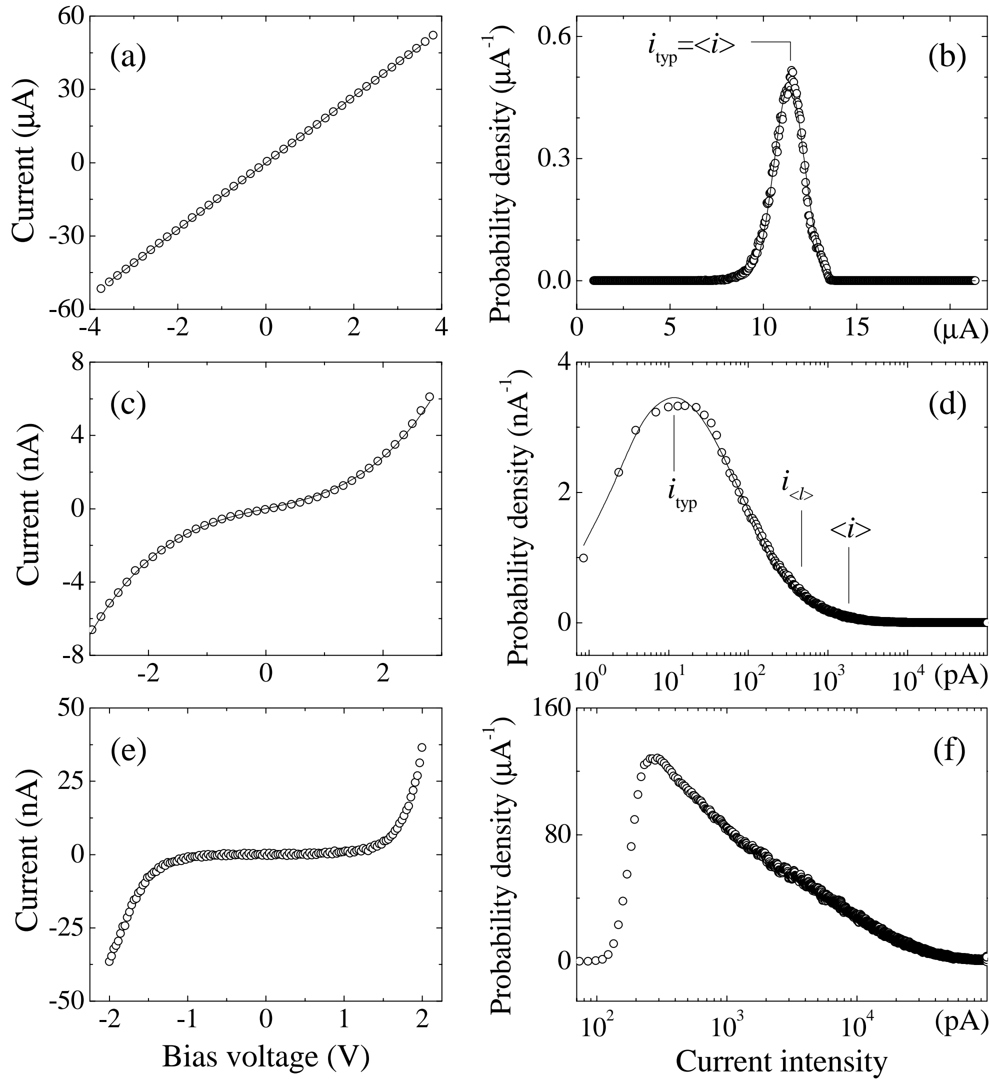

Fig. 2. (a, c, e) Examples of local current-voltage characteristics (○) measured on an oxide free Ru film (a), a Co oxide film (c) and an Al oxide film (e). The solid lines are fits according to (a) a linear law and (c) the model of reference [16]. (b, d, f) Distributions of local currents $P_i(i)$. (○) Experimental data calculated from the current images obtained on the Ru surface (b), the Co oxide surface (d) and the Al oxide surface (f) displayed in Figure 1. Solid lines: (b) Gaussian fit, (d) fit to equation (1). Notice that the typical local current i_{typ} and the average local current $\langle i\rangle$ are equal to each other for the oxide free Ru film (b), whereas they differs by two orders of magnitude for the CoO_x/metal junctions (d). (d) $i_{\langle l\rangle}$ is the local current corresponding to the average Co oxide thickness.

$P_i(i)$ is a broad distribution with a long tail extending over several decades, which allows for enormous relative fluctuations of current. These large fluctuations are a natural consequence of the exponential dependence of the tunnel transmission t with the barrier parameters. The type of current distribution is well described by a parameter B that gives a measure of the extension of the distribution $P_i(i)$: $B = (\langle i\rangle - i_{\text{typ}})/i_{\text{typ}} = \exp(3\beta^2/2) - 1$, where $\langle i\rangle = \exp(\alpha' + \beta^2/2)$ is the average local current and $i_{\text{typ}} = \exp(\alpha' - \beta^2)$ is the most probable local current also called typical current. Importantly, the fluctuation parameter β divides the thickness fluctuation σ_l by the tunneling length scale λ, and not by the average barrier thickness $\langle l\rangle$. Thus, barriers which are smooth according to usual criterion (small $\sigma_l/\langle l\rangle$) may nevertheless exhibit considerable current fluctuations if λ is small. Notice finally that a broad log-normal current distribution can be conveniently expressed as a power law of the form $P_i(i) \simeq C/i^{1+\mu(i)}$ with a slowly (logarithmically) varying exponent $\mu(i)$. As a consequence, the statistical properties of the local current i are effectively connected to the generalized central limit theorem of Lévy, with deviations due to the i-dependence of $\mu(i)$ [12].

The experimental current distribution of Figure 2d (cobalt oxide) is well fit using the equation (1) for $P_i(i)$, which contains only two adjustable parameters α' and β, despite slight deviations, invisible in the figure, for high current values. In comparison, the distribution of tunnel

current through Al oxide (Fig. 2f) gives a poorer fit to the log-normal law, which is not unexpected since the latter derives from fairly crude approximations (rectangular barrier, Gaussian fluctuations of barrier thickness). As the log-normal parameterization is very convenient for discussing statistical properties, we will focus in the following on results from the Co/CoO_x sample. Notice however that all of the qualitative conclusions drawn for CoO_x apply also to AlO_x.

The fit of the current distribution of the Co/CoO_x junction (Fig. 2d) gives $\alpha' = 5.84$ and $\beta = 1.84$. As shown next, these parameters can be related to the statistical properties of the Co oxide barrier. Local current-voltage curves (Fig. 2c) recorded at different sites were fit using Simmons' theory [15]. Assuming an effective contact area between the tip and the sample of 10 nm^2 (size of the smallest current features), we obtained an effective barrier height $\phi = V_0 - E \simeq 2.5$ eV and a barrier thickness $\langle l \rangle \simeq 0.9$ nm. The latter value agrees with the expected average Co oxide thickness (1.0 ± 0.5 nm as estimated from XPS). As for the barrier height value, it agrees with the 2.6 eV reported earlier [16]. It corresponds to an attenuation length $\lambda = 0.06$ nm. By combining this value with the parameter $\beta = \sigma_l/\lambda$ deduced from the fit of $P_i(i)$, we estimate the standard deviation of the barrier thickness distribution to be $\sigma_l = 0.1$ nm. The topographical roughness (0.5 nm), significantly larger than σ_l, may be mostly due to the underlying Co metal film, which would be covered by an oxide layer of almost constant thickness. This is supported by the absence of clear correlation between the topographical and current features.

Thus, we have demonstrated that relatively small spatial fluctuations of tunnel barrier thickness ($\sigma_l = 0.1$ nm) can account for the broad distributions of tunnel current observed in metal-oxide junctions. However, as we verified by calculating numerically the $P_i(i)$ distributions generated by Gaussian fluctuations of V_0, such broad distributions may also result from tiny spatial fluctuations of barrier height due to a chemical non-uniformity of the oxide films, related to the existence of several Al or Co oxidation states. Moreover, localized electronic states in the barrier due to impurities or defects, which would produce resonant electron tunneling, might also induce large spatial fluctuations of conductance [17,18]. Nevertheless, given the very small size of the barrier thickness fluctuations needed to reproduce the observed tunnel current distributions, thickness fluctuations are inevitably an important source of randomness in tunnel junctions with $\lambda \lesssim 0.1$ nm.

Whatever their physical origin, the broad current distributions evidenced here have important consequences on the transport properties of metal-oxide junctions. First, from the parameters of the distribution $P_i(i)$ determined experimentally for Co oxide (Fig. 2d), we calculate that half of the current tunneling through the barrier is transmitted by only 3% of the sample surface area. In other words, the tunnel current flows in such an inhomogeneous manner through the oxide barrier that the total conductance of the junction is dominated by contributions from very few sites with relatively high transmissions. This domination of the tunnel transport by a few tunneling paths is likely to play a role in other tunneling problems [9]. For instance, it is compatible with the striking efficiency of the "pathway strategy" to calculate how electrons tunnel between redox groups in complex proteins by taking into account only the most direct coupling route, among thousands, between donors and acceptors [10].

Second, the usual macroscopic measurements performed on tunnel junctions which yield only average values must be handled very cautiously in the presence of broad distributions. For instance, a capacitance measurement usually gives the average barrier thickness $\langle l \rangle$. From this, one may be tempted to deduce that the local tunnel current is $i_{\langle l \rangle} = 4A\eta^{-1}\exp(-\langle l \rangle/\lambda) = \exp(\alpha')$. This value is however neither close to the typical current value $i_{\mathrm{typ}} = i_{\langle l \rangle}\exp(-\beta^2)$ nor to the average current value $\langle i \rangle = i_{\langle l \rangle}\exp(\beta^2/2)$ (Fig. 2d). Concomitantly, a macroscopic measurement of the tunnel current, yielding only $\langle i \rangle = \exp(\alpha' + \beta^2/2)$, fails to fully characterize the tunnel barrier if one is not able to determine separately α' or β. In particular, $\langle l \rangle$ cannot be readily deduced from such a measurement.

Finally, broad distributions of local current imply an unusual variation of the typical current density with the surface area of the junction. In usual cases, the total current flowing through a conductor is proportional to the surface area S of the conductor. Hence, the current density is independent of S. This intuitive result may appear as general. However, it assumes implicitly that the local current distributions are narrow. Interestingly, in the case of broad current distributions, this result does not hold any more and the statistical properties of the current density depend strongly on the scale at which the current density is evaluated.

Indeed, let us consider the current density $J(S)$ averaged over a surface area S. Theoretically, the probability distribution of $J(S)$ can be deduced from successive convolutions of $P_i(i)$ with itself [12]. The most probable value of $J(S)$ is called the typical current density $J_{\mathrm{typ}}(S)$. For small S, broad distributions of local current give rise to broad distributions of $J(S)$. This implies non reproducible transport properties for small tunnel junctions. Moreover, as the distribution of $J(S)$ strongly changes with increasing S (insert of Fig. 3), $J_{\mathrm{typ}}(S)$ varies significantly with S. However, for sufficiently large S, the fluctuations of local current eventually average out so that the distributions of $J(S)$ become narrow (quasi-Gaussian), as seen in the insert of Figure 3. Then, the transport properties of the junctions get reproducible and, simultaneously, $J_{\mathrm{typ}}(S)$ becomes independent of S. The quantity $J_{\mathrm{typ}}(S)$ should be proportional to i_{typ} for small samples and proportional to $\langle i \rangle$ for large enough ones [12]. Therefore, $J_{\mathrm{typ}}(S)$ is expected to increase with increasing S by a factor of $\langle i \rangle / i_{\mathrm{typ}} = (1 + B) = \exp(3\beta^2/2)$.

To check if this unusual increase really occurs, we have extracted from the large 150×150 nm^2 current image of Figure 1d, made of 512×512 pixels, sets of smaller images of sizes $N = n \times n$ pixels, with n ranging from 1 to 128, and determined the typical current density $J_{\mathrm{typ}}(S)$

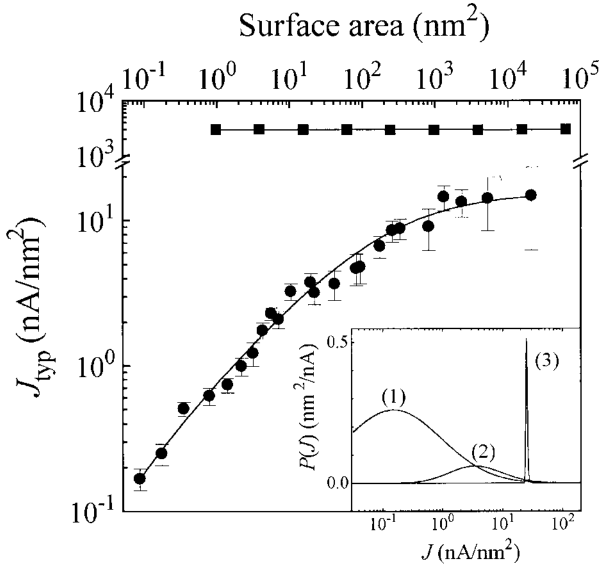

Fig. 3. Variation of the typical current density $J_{\rm typ}(S)$ with the surface area S for a metal-insulator Co/CoO$_x$ junction (●) and a metallic Ru film (■), as deduced from the current images of Figure 1. The solid lines are guides for the eye. Insert: probability distributions $P(J)$ of current density $J(S)$ calculated from the log-normal model of the current distribution $P_i(i)$ (Fig. 2d), for three different sample surface areas, (1) $S = 0.3 \times 0.3$ nm^2, (2) $S = 1.2 \times 1.2$ nm^2 and (3) $S = 53 \times 53$ nm^2.

for each of the corresponding S. Remarkably, we find indeed that $J_{\rm typ}(S)$ increases by a significant factor of 90 [19] as S varies from 10^{-1} to 2×10^4 nm^2. This experimental variation shown in Figure 3 agrees with the theoretical expectations [12], with small quantitative differences due to spatial correlations [20] of the tunnel currents and truncation effects. Notice that the same treatment applied to the current data measured on the Ru film (Fig. 1b), which presents a narrow current distribution, leads, as expected, to an utterly size-independent typical current density (Fig. 3).

An important outcome of Figure 3 is that it takes surprisingly large surface areas for the spatial fluctuations of tunnel current to fully average out, as $J_{\rm typ}(S)$ becomes almost independent of S *only* for surface areas larger than $S_X \simeq 10^3$-10^4 nm^2. For $S > S_X$, one gets a normal scaling of the resistance of tunnel junctions ($R \propto 1/S$), in agreement with measurements made so far with S in the μm^2 and high sub-μm^2 ranges [21]. For $S < S_X$, since the current density varies with S, a deviation from this normal scaling is observed. The constancy of $J_{\rm typ}(S)$ for $S > S_X$ further indicates that well-prepared tunnel junctions ($\sigma_l \lesssim 0.1$ nm) with surface areas larger than typically 100×100 nm^2 can show reproducible macroscopic properties and, even so, exhibit very large spatial fluctuations of tunnel current at scales smaller than $\sqrt{S_X}$ [22]. On the other hand, the transport properties of tunnel junctions with small barrier attenuation length ($\lambda \lesssim 1$ nm) and surface areas significantly smaller than 100×100 nm^2 can be predicted as hardly reproducible, unless barrier fluctuations can be further reduced.

Notice finally that a related self-averaging of the current fluctuations is also likely to occur at low temperatures. Indeed, as the quantum delocalization of the electrons ($\Lambda = \hbar\sqrt{2\pi}/\sqrt{Mk_{\rm B}T}$) can easily be much larger than $\sqrt{S_X}$, the transmission of *each electron* may also average out the spatial fluctuations of local tunnel transmission described here. Hence, the reproducibility, sometimes achieved, of the transport properties of large or low temperature junctions may well hide the exotic statistical properties of the tunnel current at small scales that are revealed by our high resolution current cartography experiments performed at room temperature.

This work was partially supported by the European Community Brite Euram project "Hot Spin Electronics Amplifiers for Magnetic Sensors" (BE96-3407). We thank J. Hommet for experimental contributions and M. Devoret for fruitful discussions.

References

1. Broad distributions are distributions that decay slowly at large values. When they decay as power laws, as in the cases studied by Lévy, some of their moments are infinite. P. Lévy, *Théorie de l'addition des variables aléatoires* (Gauthier-Villars, Paris, 1937).
2. For reviews see M.F. Shlesinger, G.M. Zaslavsky, J. Klafter, Nature **363**, 31 (1993); *Lévy Flights and Related Topics in Physics*, edited by M.F. Shlesinger, G.M. Zaslavsky, U. Frisch (Springer, Berlin, 1995).
3. A.O. Caldeira, A.J. Leggett, Phys. Rev. Lett. **46**, 211 (1981).
4. I. Giaever, H.R. Zeller, Phys. Rev. Lett. **20**, 1504 (1968).
5. P.W. Anderson, B.I. Halperin, C.M. Varma, Philos. Mag. **25**, 1 (1972); W.A. Phillips, J. Low. Temp. Phys. **7**, 351 (1972).
6. For a review, see D. Haarer, in *Persistent Spectral Hole-Burning*, edited by W.E. Moerner (Springer, Berlin, 1988).
7. A. Zumbusch, L. Fleury, R. Brown, J. Bernard, M. Orrit, Phys. Rev. Lett. **70**, 3584 (1993).
8. J. Colmenero, R. Mukhopadhyay, A. Alegría, B. Frick, Phys. Rev. Lett. **80**, 2350 (1998).
9. F. Ladieu, J.P. Bouchaud, J. Phys. I France **3**, 2311 (1993) and references therein.
10. J.N. Onuchic, D.N. Beratan, J. Chem. Phys. **92**, 722 (1990).
11. J.S. Moodera, L.R. Kinder, T.M. Wong, R. Meservey, Phys. Rev. Lett. **74**, 3273 (1995).
12. F. Bardou, Europhys. Lett. **39**, 239 (1997).
13. F. Houzé, R. Meyer, O. Schneegans, L. Boyer, Appl. Phys. Lett. **69**, 1975 (1996).
14. The tunnel transmission is inferred for Co oxide from the local current value and the barrier parameters derived later in the paper.
15. J.G. Simmons, J. Appl. Phys. **34**, 1793 (1963).
16. P.A. Cox, *Transition Metal Oxides* (Clarendon Press, Oxford, 1995), p. 134.

17. C.T. Rogers, R.A. Burhman, Phys. Rev. Lett. **55**, 859 (1985).
18. E.Y. Tsymbal, D.G. Pettifor, Phys. Rev. B **58**, 432 (1998).
19. The finite spatial resolution of the experimental setup might result in an underestimate of this factor. See following note.
20. The autocorrelation function of the current image of Figure 2d exhibits two different length scales. First, there is a small length scale $L_1 \lesssim 0.3$ nm, which is approximately equal to the size of one pixel. This length scale also appears in the autocorrelation function of the topographic image of Figure 2c. Then, we attributed it to the finite resolution of the images. Second, there is a larger length scale $L_2 \simeq 6.5$ nm which we attribute to structures in the oxide layer, visible in the image. This length scale does not appear in the topographical image of Figure 2c. Thus, the current cartography presented here offers the opportunity to study buried structures that are invisible in usual AFM topographical measurements and that deserve further study. Note at last that the combination of L_1 and L_2 results in some "oscillations" around the global scaling of the current $J_{\rm typ}(S)$ with the surface area S. Moreover, the plateau exhibited by $J_{\rm typ}(S)$ around 40 nm^2 corresponds to the second length scale ($L_2^2 \simeq 40$ nm^2).
21. See *e.g.* W.J. Gallagher *et al.*, J. Appl. Phys. **81**, 3741 (1997).
22. Beware that if the barrier thickness fluctuations were only slightly larger, then S_X would increase drastically as shown in reference [12]. For instance, $\sigma_l = 0.2$ nm would correspond to $S_X = 1\ \mu$m^2. Hence, the domination of the tunnel transport by few tunneling paths may well extend up to the scale of the junctions itself and apply to the total current flowing through the junctions. This would imply non-reproducible macroscopic properties of the junctions, even in the μm^2 range.